Journal of Medicinal Chemistry

Article

pubs.acs.org/jmc

Evaluation of ^{18}F-Labeled Benzodioxine Piperazine-Based Dopamine D_4 Receptor Ligands: Lipophilicity as a Determinate of Nonspecific Binding

Fabian Kügler,[†] Wiebke Sihver,[†] Johannes Ermert,[†] Harald Hübner,[‡] Peter Gmeiner,[‡] Olaf Prante,[§] and Heinz H. Coenen*,[†]

[†]Institute of Neuroscience and Medicine, INM-5, Nuclear Chemistry, Forschungszentrum Jülich GmbH, Jülich, Germany

[‡]Department of Chemistry and Pharmacy and [§]Laboratory of Molecular Imaging, Friedrich-Alexander University, Erlangen, Germany

ABSTRACT: Derivatization of the putative neuroleptic 1-(2,3-dihydrobenzo[1,4]dioxin-6-yl)-4-(4-fluorobenzyl)-piperazine (**3a**) led to a series of new dopamine receptor D_4 ligands displaying high affinity (K_i = 1.1−15 nM) and D_2/D_4 subtype selectivities of about 800−6700. These ligands were labeled with the short-lived positron emitter fluorine-18 and analyzed for their potential application for imaging studies by positron emission tomography (PET). In vitro autoradiography was used to determine their nonspecific binding behavior as a result of their structural and thus physicochemical properties. The biodistribution, in vivo stability, and brain uptake of the most promising D_4 radioligand candidate were determined. This proved to be 1-(2,3-dihydrobenzo[*b*][1,4]dioxin-6-yl)-4-((6-fluoropyridin-3-yl)methyl)piperazine ([^{18}F]**3d**), which revealed an excellent binding pattern with a high selectivity and limited nonspecific binding in vitro. This analogue also exhibited a high stability and an extremely high brain uptake in vivo with specific binding in hippocampus, cortex, colliculus, and cerebellum as determined by ex vivo autoradiography. Thus, [^{18}F]**3d** appears as a suitable D_4 radioligand for in vivo imaging, encouraging continued evaluation by PET studies.

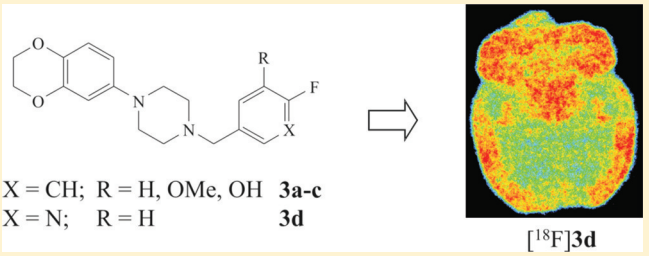

INTRODUCTION

From the five known subreceptors of the dopaminergic system the D_4 receptor exhibits a specific pharmacological profile,[1,2] and an extensive scope of polymorphism of the human dopamine receptor D_4 (DRD4) gene is known.[3,4] It is attributed to an extremely low density in brain.[5,6] Therefore, there is still ambiguity about physiological and pathophysiological functions as well as exact localization and distribution density of this subtype,[7,8] although the dopamine D_4 receptor was first cloned in 1991.[1] Immunohistochemistry and in vitro hybridization led to contradictory findings and differences between species but implicated an expected higher expression of D_4 in the prefrontal cortex and the limbic system and also in the temporal cortex, parts of tectum, and cerebellum.[7−11]

The D_4 receptor became of more interest, since it had become clear that the atypical neuroleptic clozapine showed a 10-fold higher affinity for D_4 than for D_2 receptor.[1] Therefore, higher efficacy of clozapine to nonresponders as well as to therapy of negative symptomatology was discussed as a consequence of D_4 binding. The fact that further studies did not reproducibly confirm a direct relation between schizophrenia and the D_4 receptor density,[12,13] which could also be a result of a lack of true D_4 antagonists, indicated that the role in psychiatric diseases remains questionable. Nevertheless, up to now various subtype selective ligands were developed for the D_4 receptor.[14,15] From *N*-([4-(2-cyanophenyl)piperazin-1-yl]-methyl)-3-methylbenzamide (PD-168077),[16] one of the first selective D_4 agonists developed by Glase in 1997, up to various D_4-selective compounds developed by Gmeiner's group including 2-[4-(4-chlorophenyl)piperazin-1-ylmethyl]pyrazolo-[1,5-*a*]pyridine (FAUC 213)[17] and the benzoimidazole 2-[4-(3,4-dimethylphenyl)piperazin-1-ylmethyl]-1*H*-benzoimidazole (A-381393),[18] the basic structure consists of a piperidine or, in most cases, a piperazine backbone with two nitrogen-linked aromatic rings, one of them being an arylamine. The D_4 subtype selectivity of compounds under investigation is strongly dependent on the presence of a methylene linker that defines the distance between the piperazine ring and the lipophilic moiety. The relation between structure and binding behavior was meanwhile also substantiated by CoMFA studies and integrated in a pharmacophore model.[17,19]

A variety of D_4 agonists showed a proerectile effect in animal experiments,[20,21] thereby confirming the role of D_4 receptors on the physiology of sexual functions. It is assumed that differences in haplotypes of the D_4 receptor that show a wide range of polymorphic tandem repeats of the third cytoplasmic loop are responsible for libido dysfunctions and for other neurobehavioral disorders like attention deficit hyperactivity disorder, novelty seeking, and substance abuse.[22] Different

Received: June 14, 2011
Published: October 31, 2011

Scheme 1. General Synthetic Scheme of Title Structures and Reference Compounds[a]

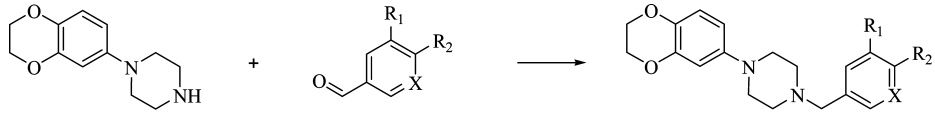

1

2a: X= CH, R_1 = H, R_2 = F
2b: X= CH, R_1 = OMe, R_2 = F
2c: X= CH, R_1 = OH, R_2 = F
2d: X= N, R_1 = H, R_2 = F

3a: X= CH, R_1 = H, R_2 = F
3b: X= CH, R_1 = OMe, R_2 = F
3c: X= CH, R_1 = OH, R_2 = F
3d: X= N, R_1 = H, R_2 = F

[a]Reaction conditions: CH_3OH, CH_3COOH, $NaBH_3CN$, 60 °C, 24 h.

binding porperties of D_4 ligands with respect to the distinct D_4 receptor polymorphism have been attested.[23]

Noninvasive imaging using selective radioligands for the D_4 receptor by positron emission tomography (PET) or single photon emission computer tomography (SPECT) provides in principle the opportunity to investigate the D_4 receptor expression in the living human brain with high sensitivity. From the existing radioligands to determine D_4 activity in brain, tritiated ligands like 2-{4-[(2-[^{3}H]phenyl-1*H*-imidazol-4-yl)-methyl]piperazin-1-yl}pyrimidine ([^{3}H]NGD 94-1)[24] are of course not applicable for in vivo imaging, while other suitably labeled candidates require the blockade of interfering receptor subtypes because of their insufficient selectivity, as shown by Boy et al.[25] Another major problem is the inadequate ratio of specific to nonspecific and unspecific binding,[26,27] which is most obtrusive because of the very low D_4 receptor density. A decrease of specific binding to non-D_4 receptors (unspecific binding) could be reached by a better understanding of the above-mentioned structure−activity relationship (SAR) which led to ligands with high affinity and selectivity.[19,28] However, the nonspecific binding of D_4 radioligand candidates, such as binding to brain lipids which is hardly reversible and barely displaceable by nonradioactive ligands, has not yet been considered adequately by SAR studies and is difficult to predict. It is anticipated that nonspecific binding correlates with the lipophilicity of the substance. In fact, such a correlation is sometimes observed,[29−31] and in a recent study on analogues of *β*-carboline harmine[32] a similar comparison of in vitro data and lipophilicity was performed.

As a typical D_4 ligand lead structure, according to SAR findings, the fluorinated D_4 antagonist 1-(2,3-dihydrobenzo-[1,4]dioxin-6-yl)-4-(4-fluorobenzyl)piperazine **3a** shows an outstanding subtype selectivity of D_2/D_4 > 5000.[33] The aim of the present study was to determine the suitability of this compound to act as a D_4 receptor ligand for imaging studies, when labeled with fluorine-18. Further derivatives of the lead compound were developed and studied for their dopamine receptor affinities and functional activity and with special interest on the determination of specific to nonspecific binding ratios by means of in vitro autoradiography. As predicted from the in vitro data, the most suitable radioligand was selected for determination of its biodistribution, in vivo stability, and brain uptake. Together with the in vitro and ex vivo radioligand autoradiography, the results were evaluated in order to assess the suitability of a new D_4 radioligand candidate for in vivo imaging.

RESULTS AND DISCUSSION

Ligands and ^{18}F-Labeled analogues. Continuing the efforts on the development of ^{18}F-labeled D_4 selective radioligands for in vivo use[34] led to ^{18}F-labeling of 2-(4-(4-fluorophenyl)piperazin-1-ylmethyl)indole-5-carbonitrile (FAUC 316). However, preliminary studies showed that its use as in vivo radioligand failed because of its high lipophilicity. Thus, dihydrobenzo[1,4]dioxine-1-(2,3-dihydrobenzo[1,4]-dioxin-6-yl)-4-(4-fluorobenzyl)piperazine (**3a**) was chosen as alternative lead structure with the goal to develop less lipophilic derivatives while maintaining the affinity, and three new derivatives thereof were synthesized and chemically characterized according to Scheme 1.

Analogous to the description of Liu et al.,[35] the intermediate 1-(1,4-benzodioxine-6-yl)piperazine (**1**) was synthesized via cyclization of the commercially available aminodioxine 2,3-dihydrobenzo[*b*][1,4]dioxin-6-amine with bis(2-chloroethyl)-amine hydrochloride.[36] Reductive amination with the appropriate aldehydes **2a−d** led to a series of new 3-substituted 6-(4-[4-fluorobenzyl]piperazine-1-yl)benzodioxine derivatives obtained in 20−85% yield. They all were used as reference compounds for chromatographic identification of radioactive products, for determining their molar activities, and as competitors for autoradiographic evaluation studies. The ^{18}F-labeled ligands were obtained in no-carrier-added form by the same buildup syntheses starting with nucleophilic substitution with nca [^{18}F]fluoride of analogous benzylaldehydes **2a−c** as precursors, where R_2 represents the trimethylammonium triflate moiety (-$NMe_3^+TfO^-$), or chlorine in the case of **2d**, as aromatic leaving group. Optimization of labeling conditions, comprising variation of temperature, solvent, and anion activating system, is given elsewhere together with details on the syntheses of standards, intermediates, and precursors for radiofluorination.[36] The radiochemical yields of the products [^{18}F]**3a−d** obtained after both reaction steps, i.e., radiolabeling and subsequent amination, are summarized in Table 1. In the first step the nca labeled fluoroaldehydes [^{18}F]**2a−d** were obtained with radiochemical yields of 72−80%.

Table 1. Total Radiochemical Yields of [^{18}F]3a−d after Radiofluorination and Amination in a One-Pot Reaction

[^{18}F] fluoroaldehyde	final product	radiochemical yield (%)	total synthesis time (min)
[^{18}F]**2a**	[^{18}F]**3a**	35 ± 5	~90
[^{18}F]**2b**	[^{18}F]**3b**	20 ± 5	~90
[^{18}F]**2c**	[^{18}F]**3c**	9 ± 4	~120
[^{18}F]**2d**	[^{18}F]**3d**	15 ± 5	~80

In contrast to the macroscopic synthesis of the ligands, the reductive amination with the nca intermediate [^{18}F]fluoro-aldehydes could also be performed in DMSO instead of methanol. Labeling and amination could therefore be performed as one-pot reaction. The nonsubstituted and the methoxy compound ([^{18}F]**3a** and [^{18}F]**3b**) were generated in

dx.doi.org/10.1021/jm200762g | *J. Med. Chem.* 2011, 54, 8343−8352

Table 2. Binding Affinities of the Derivatives 3a–d to the Human Dopamine Receptor Subtypes D_{2long}, D_{2short}, D_3, and $D_{4.4}$, the Porcine D_1 Receptor, and the Porcine 5-HT_{1A}, 5-HT_2, and α_1 Receptors

		$K_i \pm$ SD (nM)[a]							
compd	R	$hD2_{long}$[b]	$hD2_{long}$[b]	hD_3[b]	$hD_{4.4}$[b]	pD_1[c]	p5-HT_{1A}[d]	p5-HT_2[e]	pα_1[f]
3a	H	7600 ± 570	5700 ± 1300	3900 ± 71	1.1 ± 0.56	19000 ± 11000	5200 ± 2200	7000 ± 5700	4000 ± 780
3b	OMe	17000 ± 1400	16000 ± 2100	5900 ± 640	4.2 ± 0.071	23000 ± 4200	5600 ± 2100	4200 ± 2100	3300 ± 350
3c	OH	9000 ± 1100	6100 ± 71	4200 ± 1300	7.3 ± 2.6	15000 ± 3600	6200 ± 710	2300 ± 640	3000 ± 210
3d		29000 ± 2000	45000 ± 710	17000 ± 710	15 ± 0.71	35000 ± 4200	21000 ± 2100	5800 ± 2100	11000 ± 710

[a] K_i values are the mean values of two independent exrperiments each done in triplicate. [b] [^{3}H]spiperone. [c] [^{3}H]**5**. [d] [^{3}H]**4**. [e] [^{3}H]ketanserin. [f] [^{3}H]prazosin.

good radiochemical yields of 20–35% after HPLC separation and with molar activities of about 60 GBq/μmol. Since no labeling yield could be observed using the trimethylammonium precursor of the hydroxy compound [^{18}F]**2c**, the benzyloxy analogue was used instead. Therefore, the low RCY of only 9% and a molar activity of only 30 GBq/μmol for [^{18}F]**3c** were due to the additional step necessary for cleaving the benzyl protecting group. [^{18}F]Fluoropyridine ([^{18}F]**2d**) is sensitive to degradation; thus, the RCY and molar activity of radioligand [^{18}F]**3d** were also rather low (cf. Table 1).

Receptor Binding and Intrinsic Activities. The lead compound **3a** and its derivatives 1-(2,3-dihydrobenzo[1,4]-dioxin-6-yl)-4-(4-fluoro-3-methoxybenzyl)piperazine (**3b**), 5-[4-(2,3-dihydrobenzo[1,4]dioxin-6-yl)piperazin-1-ylmethyl]-2-fluorophenol (**3c**), and 1-(2,3-dihydrobenzo[*b*][1,4]dioxin-6-yl)-4-((6-fluoropyridin-3-yl)methyl)-piperazine (**3d**) were subjected to receptor binding studies to test for their ability to displace [^{3}H]spiperone from the cloned human dopamine receptors D_{2long}, D_{2short},[37] D_3,[38] and the most common D_4 polymorphism $D_{4.4}$,[39] being stably expressed in Chinese hamster ovary (CHO) cells.[40]

Additionally, the metabotropic receptors 5-HT_{1A}, 5-HT_{2A}, and α_1, from which it is known that they could reveal competing binding affinity for putative D_4 ligands, were measured utilizing porcine cortical membranes and the selective radioligands *N*-[2-[4-(2-methoxyphenyl)-1-piperazinyl]ethyl]-*N*-(2-pyridyl)cyclohexanecarboxamide ([^{3}H]**4**, [^{3}H]-WAY100635), [^{3}H]ketanserin, and [^{3}H]prazosin, respectively.[41] The highly expressed but structurally and functionally different dopaminergic receptor D_1 was measured using porcine striatal membranes and the radioligand 7-chloro-3-methyl-1-phenyl-1,2,4,5-tetrahydro-3-benzazepin-8-ol ([^{3}H]**5**, [^{3}H]-SCH23390). The results of the receptor binding studies are presented in Table 2.

All ligands showed high affinity to D_4 in the low nanomolar range and weak affinities to all other tested receptors (Table 2). Among the series of compounds, the lead compound **3a** showed highest affinity to the D_4 receptor combined with an exceptional D_4 subtype selectivity (Table 3). The introduction of a methoxy or hydroxy group to the fluorophenyl moiety (see **3b**, **3c**) led to a minor decrease in D_4 affinity of these compounds. The displacement of the fluorophenyl group by the pyridinyl substituent **3d** induced a minor decrease in D_4 affinity by a factor of about 10. However, the D_4 subtype selectivity of >1000 (D_4/D_3) and >2000 (D_4/D_2) for **3d** was still adequate and comparable to the values of the previously described fluoro-substituted pyrazolo[1,5-*a*]pyridine.[34] The subtype selectivity was high for all derivatives (Table 3) but highest for **3a**, followed by **3b**, **3d**, and **3c**. Remarkably, **3a** displayed a K_i ratio of more than 5000 for D_2 (D_4/D_2) and 3500 for D_3 (D_4/D_3), which is, to our knowledge, one of the highest selectivities for D_4 over D_3 reported up to now.

Table 3. D_4 Subtype Selectivity within the Family of D_2-like Receptors

		ratio $K_i(D_2$ or $D_3)/K_i(D_{4.4})$		
compd	$K_i(hD_{4.4})$ (nM)	$hD_{2long}/hD_{4.4}$	$hD_{2short}/hD_{4.4}$	$hD_3/hD_{4.4}$
3a	1.1	6700	5000	3600
3b	4.2	4000	3800	1400
3c	7.3	1300	830	590
3d	15	2000	3000	1100

In addition, the data on receptor affinities of the series of compounds with functional data were extended using our previously described mitogenesis assay.[42] The agonist activation of dopamine receptors is known to increase mitogenesis in heterologously transfected cell lines, measuring the rate of proliferation in growing cells.[43] Since agonist ligands preferentially bind to the active GPCR conformation (high-affinity state) and antagonists have equal affinity for the active and inactive state, it is important to determine the intrinsic activity for a putative radioligand. These data could also help to interpret differences between agonist and antagonist radioligands in the in vivo binding behavior. Therefore, we investigated the intrinsic activity of the series of title compounds by measuring the [^{3}H]thymidine incorporation into growing CHO cells stably expressing the dopamine D_4 receptor.[43] In fact a neutral antagonism was determined for all title compounds under investigation in comparison with the full agonist quinpirole as a reference.

Because of the promising high D_4 receptor affinity and distinct D_4 receptor subtype-selectivity of **3a**, **3b**, **3c**, and **3d**, the radiosyntheses of the corresponding ^{18}F-labeled antagonist radioligands appeared attractive.

Pharmacology. High selectivity, good uptake and retention, stability, and low unspecific and nonspecific binding in the target tissue are key requirements for the suitability of radioligands in PET studies. While most features can be tested with the unlabeled compounds, there is little indication for their nonspecific binding behavior prior to labeling. This may be one reason why the latter is often a knockout criterion for many radiotracers that fulfill the former requirements. The radioligand [^{18}F]**3a** failed in this respect, since it exhibited a nonspecific binding of >90%. The apparent lipophilicity of **3a** prompted us to increase the hydrophilicity, resulting in the design of title compounds **3b–d**. The results from in vitro competition experiments of all derivatives directed the selection of a promising radioligand for further in vivo studies.

Lipophilicity. As an adequate estimation of this physicochemical property, the MarvinSketch 5.1.4 software[44] and the ALOGPS 2.1 software[45] were used to calculate log *P* values,

dx.doi.org/10.1021/jm200762g | J. Med. Chem. 2011, 54, 8343–8352

Table 4. Calculated and Experimental log $P_{7.4}$ of the Derivatives 3a−d

parameter	3a	3b	3c	3d
calcd MarvinSketch	3.35	3.09	2.87	2.49
calcd ALOGPS	3.23 ± 0.27	3.11 ± 0.45	2.81 ± 0.37	2.26 ± 0.32
exptl HPLC	2.71 ± 0.03	2.44 ± 0.07	1.70 ± 0.15	2.02 ± 0.17
exptl octanol/buffer	nd	2.33 ± 0.09	1.78 ± 0.01	1.81 ± 0.05

which were estimated to be between 2.3 and 3.4 (Table 4). The two different algorithms showed similar results. However, experimental log *P* values, ranging from 1.7 to 2.7, were clearly lower than the theoretical ones. Experimental values were also obtained by two different methods at pH 7.4, i.e., shake flask and HPLC method, according to the OECD guidelines for the testing of chemicals.[46] The obtained log *P* values were determined to be between 2 and 3, a range that is proposed for ligands to penetrate the blood−brain barrier, suggesting sufficient brain uptake of the corresponding radioligands.

Autoradiography. A high ratio of nonspecific to specific binding is the main reason for radiotracer failure in vivo. In this work the nonspecific binding of the radioligands was determined by using an excess of the corresponding non-radioactive reference ligand. Since a predominant contribution to nonspecific binding is the binding to phospholipids, the degree of nonspecific binding is often related to the lipophilicity of compounds. The reason why this correlation cannot be generally applied to all radioligands may be due to possible structural influences of small molecules on lipid bilayers.[47] In fact, the mechanism of nonspecific binding is still not completely understood.

After determination of suitable affinity and subtype selectivity to the D_4 receptor for all tested ligands, in vitro autoradiography studies on horizontal rat brain slices were performed with the ^{18}F-labeled radioligands to compare the nonspecific binding values with the lipophilicity (Figure 1). For this, nonspecific binding was defined as bound ^{18}F-labeled compounds in the presence of an excess of the nonradioactive ligands **3a,b** and **3c,d**, respectively. No differences in blocking behavior could be found between blocking with the authentic reference compound or with one of the other ligands. Thereby, the postulated relationship[30,31,33] between nonspecific binding and lipophilicity was found (Figure 1).

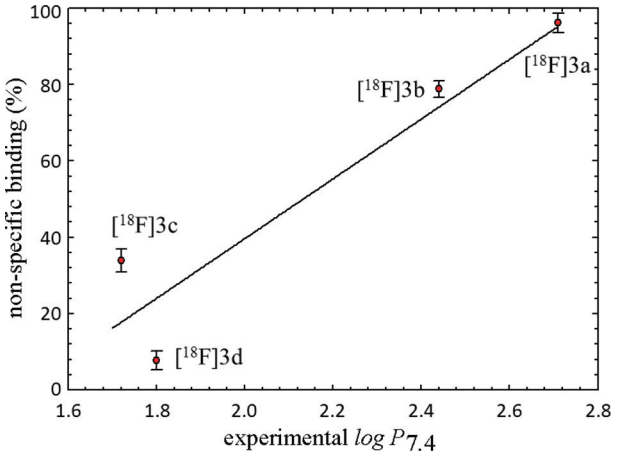

Figure 1. Relation of experimentally determined log $P_{7.4}$ values of the derivatives **3a−d** and the nonspecific binding of the ^{18}F-labeled compounds obtained by blocking studies with the nonradioactive standards on Wistar rat brain slices in vitro.

The more lipophilic radioligands [^{18}F]**3a** and [^{18}F]**3b** showed unacceptable high nonspecific binding of 96% and 79%, respectively, and seem therefore not suitable as radiotracers. In contrast, nonspecific binding of [^{18}F]**3c** was only 33%, and [^{18}F]**3d** showed even a lower degree of nonspecific binding of only 7%. Although [^{18}F]**3d** exhibited a lower D_4 affinity than the other ligands, it lends itself to further ex vivo studies because of its high selectivity and low nonspecific binding.

In vitro autoradiography studies of the more hydrophilic compounds [^{18}F]**3c** and [^{18}F]**3d** showed generally a specific binding throughout the whole rat brain. Both radioligands displayed a distinct high accumulation in the colliculus and in the medial nuclei of the cerebellum. As presented in Figure 2a, there is no marked higher accumulation in hippocampus, frontal cortex, and striatum. By contrast, in ex vivo autoradiography studies with NMRI mice using [^{18}F]**3d**, high binding was observed in cortex and hippocampus (Figure 2b). In comparison with the cresyl violet stained image of the same slice, the good contrast allows differentiation between the outer layers of cortex with high binding and lower binding in middle layers of cortex. In the hippocampus high binding uptake was observed in dentate gyrus (GD) and cornu ammonis 3 (CA3). This is in agreement with findings of Prante et al.[34] who described a significant higher uptake in the GD of rat brain slices with a ^{18}F-labeled pyrazolo[1,5-*a*]pyridine D_4 ligand but not in the other regions of hippocampus. High uptake in vitro and ex vivo was observed in regions of the colliculus. This part of brain, responsible for sorting of optical and acoustical information, was described as a region where the D_4 receptor should be found[7] but often not mentioned as a region of interest. Otherwise, the high accumulation of [^{18}F]**3d** in the cerebellum is contrary to the estimated D_4 distribution in brain, although there is information in the literature on D_4R expressing genes that are also found there.[7] However, negligible uptake of [^{18}F]**3d** was observed in striatum, which is in accordance with the low striatal D_4 receptor density in rats.[6]

In order to exclude that different binding of [^{18}F]**3d** in vitro and in vivo might be due to differences of species, in vitro autoradiography of NMRI mouse brain slices was also performed. Even though a slightly higher binding in cortex was recognizable here, the contrast of radioligand accumulation was worse in comparison to the ex vivo autoradiographs. Possible reasons for that finding could be a metabolisation by a contingent disposal of enzymes in vitro or by the incubation buffer used; however, both explanations were rendered false by experiment. Thus, it was assumed that considerable binding to intracellular components that are only accessible in vitro may result in a higher nonspecific background. For a comparison with an autoradiography from the rare literature showing results with D_4 ligands, sagittal mouse brain slices were chosen and the ex vivo binding distribution was compared with rat brain slices of the ^{131}I-labeled derivative of 3-(4-(4-chlorophenyl)-

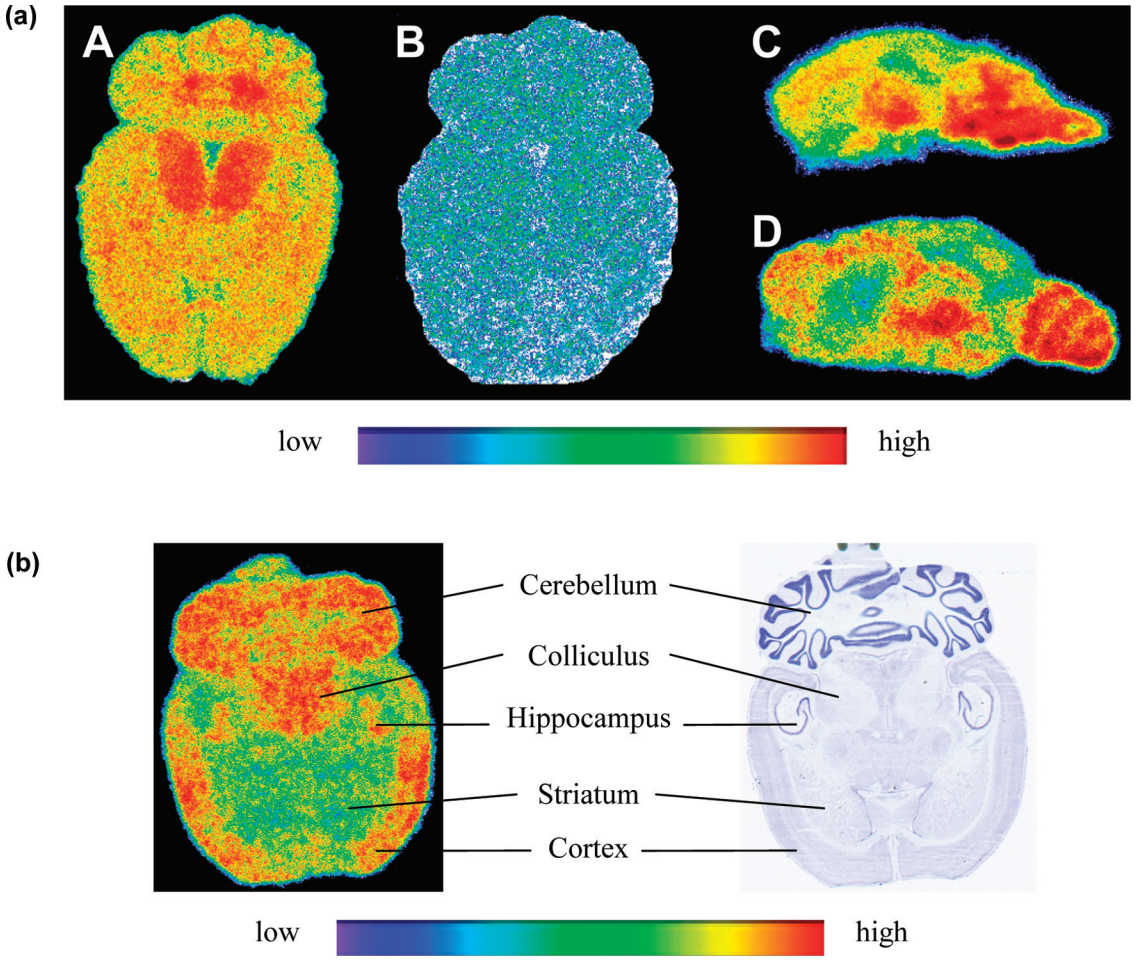

Figure 2. (a) In vitro autoradiography of a rat brain (A) with 5 nmol/L [^{18}F]**3d** and after blocking with 10 μM **3d** (B) to show nonspecific binding. Sagittal slices of in vitro (C) and ex vivo (D) autoradiography studies of mouse brain with [^{18}F]**3d**. (b) Ex vivo autoradiography (left) of horizontal planes of a mouse brain 15 min after injection of [^{18}F]**3d** and the corresponding histological image stained with cresyl violet (right).

Table 5. Biodistribution Data of [^{18}F]3d in NMRI Mice (n = 3) after Intravenous Injection

	% ID/g tissue			
	5 min	10 min	15 min	30 min
brain	4.93 ± 1.58	2.85 ± 0.14	2.27 ± 0.17	1.47 ± 0.15
heart	1.80 ± 1.00	0.52 ± 0.04	0.58 ± 0.31	1.13 ± 0.35
lung	12.99 ± 2.53	4.84 ± 1.21	4.79 ± 0.68	2.68 ± 0.80
liver	4.13 ± 1.76	6.78 ± 0.28	5.67 ± 0.30	7.79 ± 0.39
kidney	8.23 ± 2.85	5.86 ± 0.62	4.67 ± 0.40	6.03 ± 0.61
spleen	4.42 ± 1.62	3.60 ± 0.15	3.19 ± 0.20	3.13 ± 0.18
intestine	2.16 ± 0.70	2.68 ± 0.19	2.51 ± 0.39	4.47 ± 0.20
pancreas	8.36 ± 3.55	11.10 ± 0.37	6.88 ± 1.44	7.43 ± 0.56
bone	2.03 ± 0.51	2.54 ± 0.33	2.70 ± 0.89	0.93 ± 1.05
blood, final	1.62 ± 0.14	1.29 ± 0.16	1.23 ± 0.33	0.53 ± 0.21

piperazinylmethyl)pyrazolo(1,5-*a*)pyridine (FAUC113) (K_i = 2.6 nM).[48] In both studies similar binding was found in cortex and thalamus, which affirms binding in the limbic system. Also, cerebellar binding of [^{18}F]**3d** was in accordance with that previous work.

Biodistribution and in Vivo Stability. For biodistribution studies on [^{18}F]**3d** the three NMRI mice were each sacrificed at 5, 10, 15, and 30 min pi. Because of the low lipophilicity of the ligand, there was a rapid accumulation in the kidney. As expected, the hepatic uptake was lower (cf. Table 5). The high accumulation in the pancreas that even exceeded the kidney uptake attracted attention. This observation may be explained by the reported D_4 receptor expression in pancreatic β cells.[49] A high penetration of the blood–brain barrier was observed in spite of a log P of 1.8 with a brain uptake of 4.93% ID/g tissue after 5 min. After 30 min there was still more than 1% ID/g in the brain. The data showed a consistent decrease (Figure 3); thus, no compartment-trapping might be responsible for the high uptake.

In vivo stability of the radioligand [^{18}F]**3d** in the blood of mice was checked by thin layer chromatography (TLC) on aluminum oxide layers. To ensure that all potential metabolites

dx.doi.org/10.1021/jm200762g | J. Med. Chem. 2011, 54, 8343–8352

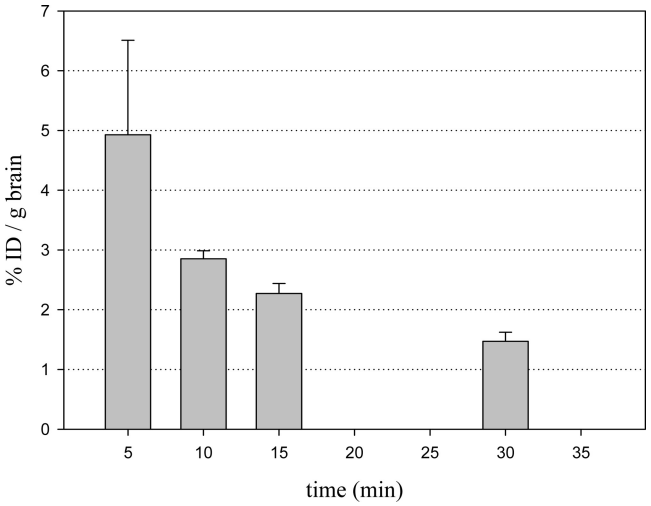

Figure 3. Time dependence of uptake of [^{18}F]**3d** in brain of NMRI mice after iv injection.

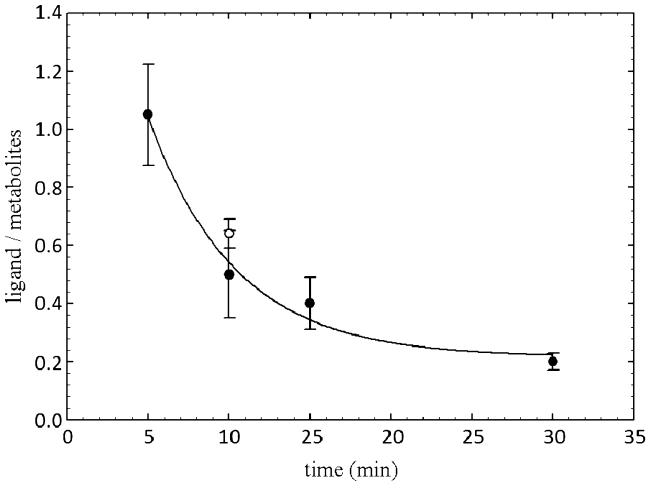

Figure 4. In vivo stability of [^{18}F]**3d** in blood plasma of NMRI mice measured by radio-TLC. The open circle point shows the result of the experiment with a higher dilution of analyzed plasma extract from which was known that all measured activity except from the radioligand-spot was from true metabolites and was not from artifacts.

are analyzed, the whole blood and plasma activity were compared as well as plasma activity and that of plasma extract.

After centrifugation of the blood, about 27% of radioactivity was found in the cell pellet. After deproteination of the plasma nearly all radioactivity remained in the serum fraction (>98%). TLC analysis of this on silica gel plates with the chosen solvent (ethyl acetate/methanol/diethylamine, 96:2:2) showed only two fractions, one remaining on the origin indicating the hydrophilic character of the corresponding compound(s) and that of the radioligand. Furthermore, it is suggested that defluorination did not take place to a considerable extent because of the very low bone uptake at all time points pi (see Table 5). The half-life of in vivo stability in blood was about 6 min.

Metabolization in brain was measured 10 min after intravenous injection in the same way but using a higher dilution with acetonitrile during the extraction step, feasible by using higher amounts of radioactivity. In mouse brain, no metabolisation of [^{18}F]**3d** after 10 min pi was detected. Analyzing the blood plasma of the same animals and also using a high dilution during extraction led to metabolite findings comparable to those before.

Therefore, it is expected that the obtained in vivo stability curve of [^{18}F]**3d** (Figure 4) does not contain "pseudo-metabolites" (artifacts), which may occur by retention of the radioligand by the remaining dried proteins. It can be assumed that the different metabolization rate indicated was due to a small degeneration of the ligand on thin layer plates, which only occurs under no-carrier-added (nca) conditions and which is rapid on silica but moderate on Alox plates. This additional degeneration of the nca product [^{18}F]**3d** on TLC plates was determined at contact times of 0, 5, 15, and 30 min (n = 3). The observed half-lives of degeneration on silica were about 15 min only but about 50 min on aluminum oxide. This is why the latter was used for all radio-TLC analyses.

CONCLUSION

Three derivatives of 1-(2,3-dihydrobenzo[1,4]dioxin-6-yl)-4-(4-fluorobenzyl)piperazine (**3a**) were characterized as high-affinity D_4 ligands with substantial D_4 selectivity in vitro. It was observed that ortho-substitution of the carbon-linked aryl moiety caused no major influence on the binding profile. The series of derivatives were labeled with fluorine-18 and analyzed for their suitability to act as D_4 radioligands, focusing on the determination of their nonspecific binding. Accordingly, there is a significant correlation between the log $P_{7.4}$ values of the derivatives and the extent of nonspecific binding as determined by competition experiments in vitro. The determined nonspecific binding of 33% and 7% of the two new derivatives [^{18}F]**3c** and [^{18}F]**3d**, respectively, is within an acceptable range.

The brain distribution of the radioligand [^{18}F]**3d** in mice determined ex vivo was essentially in accordance with literature data on D_4 receptor distribution except for an unexpected high cerebellum uptake. However, it seems to be no decisive handicap that in vitro autoradiographic studies partially showed a different binding behavior. Nevertheless, rare and contradictory data on D_4 receptor density from literature make it difficult to compare distribution of [^{18}F]**3d** with other radioligands for D_4.

The radioligand [^{18}F]**3d** showed an extremely high brain uptake in mouse brain, a moderate plasma metabolization rate, but no metabolites in the brain. All in all it can be assumed that [^{18}F]**3d** might be a suitable D_4 radioligand for in vivo imaging studies, which encourages continued evaluation in preclinical animal models by PET.

MATERIALS AND METHODS

Materials. All chemicals and p.a. solvents were purchased from Aldrich (Steinheim, Germany) or Fluka (Buchs, Switzerland) and used without further purification.

Sep-Pak C-18 Plus cartridges were purchased from Waters (Eschborn, Germany). EN cartridges and Li-Chrolut glass columns (65 mm × 10 mm) were from Merck (Darmstadt, Germany). Thin layer chromatography (TLC) was run on precoated plates of silica gel 60F254 (Merck) or alumina N. The compounds were detected by UV at 256 nm. HPLC was performed on the following system from Dionex (Idstein, Germany): an Ultimate 3000 LPG-3400A HPLC pump, an Ultimate 3000 VWD-3100 UV/vis detector (272 nm), a UCI-50 chromatography interface, an injection valve P/N 8215. Reversed-phase HPLC was carried out using a Gemini 5 mm C18 110A column, for analytical separations with a dimension of 250 mm × 4.6 mm (flow rate of 1 mL/min) and for semipreparative applications with a dimension of 250 mm × 10 mm (flow 5 mL/min), from Phenomenex (Aschaffenburg, Germany). Radio-TLC

chromatograms were analyzed by UV detection and on a Packard instant imager. All labeled ligands [^{18}F]**3a**–**d** showed a radionuclidic and radiochemical purity of >98%. ^{1}H, ^{13}C, and ^{19}F NMR spectra were recorded on a Bruker DPX Avance 200 spectrometer with samples dissolved in $CDCl_3$ or DMSO-d_6. All shifts are given in γ ppm using the signals of the appropriate solvent as a reference. Mass spectra were obtained from a Finnigan Automass Multi mass spectrometer with an electron beam energy of 70 eV. High resolution electron spray mass spectra were recorded on an LTQ FT Ultra (Thermo Fischer). Melting points are uncorrected and were determined on a Mettler FP-61 apparatus in open capillaries. Elemental analysis (CHN) results were recorded on a Leco CHNS-932 analyzer. The obtained purity for all ligands **3a**–**d** was >95%.

Chemistry. *General Procedure for Preparation of 6-(4-Benzylpiperazine-1-yl)benzodioxine Derivatives **3a**–**d**.* In a 100 mL two-neck flask 1-(1,4-benzodioxine-6-yl)piperazine (**2**) (1.816 mmol, 1 equiv) and the corresponding benzaldehyde (**2a**–**d**, 2.724 mmol, 1.5 equiv) were dissolved in 20 mL of dry methanol. After an addition of acetic acid (96%, 5.45 mmol, 3 equiv) sodium cyanoborohydride (2.724 mmol, 1.5 equiv) was added in small portions and rinsed with methanol. The mixture was heated for 12–24 h at 60 °C. After the mixture was cooled, the reaction was quenched by addition of 50 mL of saturated sodium bicarbonate solution, which was extracted three times with chloroform and washed with brine. The combined organic layer was dried over sodium sulfate and evaporated to dryness after filtration. The residue was purified by chromatography over a silica gel column (*n*-hexane/ethyl acetate, 1:2).

*1-(2,3-Dihydrobenzo[b][1,4]dioxin-6-yl)-4-(4-fluorobenzyl)-piperazine (**3a**).* **3a** was obtained as a white solid (315 mg, 0.96 mmol, 60%) from commercially available 4-fluorobenzaldehyde (**2a**) (200 mg, 1.61 mmol). Mp 120 °C. TLC (*n*-hexane/ethyl acetate, 1:2): R_f = 0.7. ^{1}H NMR ($CHCl_3$, 400 MHz) δ 2.56 (t, J = 4.8 Hz, 4H), 3.06 (t, J = 4.8 Hz, 4H), 3.50 (s, 2H), 4.19 (m, J = 4.5 Hz, 2H), 4.21 (m, J = 4.6 Hz, 2H), 6.43 (m, 2H), 6.75 (m, 1H), 6.98 (m, 1H), 7.29 (m, 2H) ppm. FT-MS (ESI): m/z 329.166 [M + H]$^+$.

*1-(2,3-Dihydrobenzo[b][1,4]dioxin-6-yl)-4-(4-fluoro-3-methoxybenzyl)piperazine (**3b**).* The methoxy derivative was obtained from the commercially available 4-fluoro-3-methoxybenzaldehyde (**2b**) (420 mg, 2.72 mmol) as a pale yellow crystalline solid (551 mg, 1.54 mmol, 85%). Mp 100 °C. TLC (*n*-hexane/ethyl acetate, 1:2): R_f = 0.44. ^{1}H NMR ($CHCl_3$, 400 MHz) δ 2.56 (t, J = 4.8 Hz, 4H), 3.06 (t, J = 4.8 Hz, 4H), 3.48 (s, 2H), 3.88 (s, 3H), 4.18 (m, J = 1.6 Hz, 2H), 4.20 (m, J = 1.6 Hz, 2H), 6.44 (m, 1H), 6.45 (m, 1H), 6.75 (m, 1H), 6.82 (m, 1H), 6.98 (m, 2H) ppm. FT-MS (ESI): m/z 359.18 [M + H]$^+$.

*5-((4-(2,3-Dihydrobenzo[b][1,4]dioxin-6-yl)piperazin-1-yl)-methyl)-2-fluorophenol (**3c**).* The hydroxyl derivative was obtained from 4-fluoro-3-hydroxybenzaldehyde (**2c**) (70 mg, 0.5 mmol) as a white crystalline solid (112 mg, 0.35 mmol, 66%). Mp 186–187 °C. TLC (*n*-hexane/ethyl acetate, 1:2): R_f = 0.35. ^{1}H NMR ($CHCl_3$, 400 MHz) δ 2.57 (m, 4H), 3.06 (m, 4H), 3.45 (s, 2H), 4.18 (m, 2H), 4.20 (m, 2H), 6.44 (m, 2H), 6.74 (m, 1H), 6.79 (m, 1H), 6.98 (m, 2H), 9.84 (br, 1H) ppm. FT-MS (ESI): m/z 345.19 (100) [M + H]$^+$.

*1-(2,3-Dihydrobenzo[b][1,4]dioxin-6-yl)-4-((6-fluoropyridin-3-yl)-methyl)piperazine (**3d**). Method A.* **3d** was obtained from 6-fluoronicotinaldehyde (**2d**) (100 mg, 0.8 mmol) as a white crystalline solid (35 mg, 0.11 mmol, 13.7%). Mp 94 °C. TLC: (chloroform/methanol, 8:1) R_f = 0.63; (ethyl acetate/methanol/diethylamine, 96:2:2): R_f = 0.78 . ^{1}H NMR ($CHCl_3$, 400 MHz) δ 2.52 (br, 4H), 3.00 (br, 4H), 3.47 (s, 2H), 4.14 (m, 2H), 4.16 (m, 2H), 6.38 (m, 2H), 6.71 (m, 1H), 6.84 (dd, J = 2.8 Hz/8.4 Hz, 1H), 7.74 (ddd, J = 2.3 Hz/8.0 Hz/8.1 Hz, 1H), 8.09 (d, J = 1.9 Hz, 1H) ppm. FT-MS (ESI): m/z 330.16 [M + H]$^+$.

*General Procedure for the Syntheses of No-Carrier-Added Labeled 6-(4-[^{18}F]Fluorobenzylpiperazine-1-yl)benzodioxine Derivatives [^{18}F]**3a**–**d**.* The nca [^{18}F]fluoride was produced via the ^{18}O(p,n)^{18}F nuclear reaction with 17 MeV protons at the JSW cyclotron BC 1710 of Forschungszentrum Juelich[50] and transferred into a dry Kryptofix 2.2.2 potassium carbonate complex by standard procedures.[51]

The corresponding trimethylammonium triflate precursor of the aldehydes **2a**,**b** (20–25 μmol), the benzyl protected trimethylammonium triflate analogue of **2c** (7 μmol) or the chloro derivative of **2d** (35 μmol) in 0.5 mL of anhydrous DMSO was added. Completion of the ^{18}F-substitution reaction was monitored by radio-HPLC (Gemini 5 μm RP18 A110, 250 mm × 4.6 mm, 1 mL/min, isocratic 60:40:0.1 v/v/v CH_3CN/H_2O/TEA). In the case of the benzyl protected derivative, palladium (black) (20 mg) and ammonium formate (250 mg) were added after radiofluorination for cleavage of protection groups to obtain [^{18}F]**2c**.

Then a solution of intermediate **1** (8.7 mg, 40 μmol) in 40 μL of acetic acid and 50 μL of DMSO and a solution of sodium cyanoborohydride (4 mg, 64 μmol) in 50 μL of DMSO were added to the radiofluorinated aldehydes. Different from the preparative amination reaction (cf. Scheme 1) DMSO at a temperature of 110 °C was used in both steps of the nca labeling process. Subsequently the reaction mixture was diluted with water and passed through a SepPak C18 cartridge, washed with water (5 mL), and dried with air. The cartridge was eluted with 1 mL of acetonitrile and the eluate injected on a semipreparative HPLC column (Gemini 5 μm RP18 A110, 250 mm × 10 mm, 4 mL/min, isocratic 30:70:0.1 v/v/v CH_3CN/H_2O/TFA). The separated fraction was diluted with 15 mL of water and passed through a second SepPak C18 cartridge. After washing with water and drying in an argon stream, the cartridge was eluted with 5 mL of diethyl ether which was evaporated in vacuo (800 up to 330 mbar) to yield dry [^{18}F]**3a**–**d**. For in vitro studies all derivatives were formulated in 300 μL of ethanol/saline (5:1) while an amount of 300 μL of saline with 1% Tween 80 was employed for ex vivo studies.

Receptor Binding Experiments. Receptor binding studies were carried out as previously described.[39] In brief, the dopamine D_1 receptor assay was done with porcine striatal membranes at a final protein concentration of 30 μg/assay tube and the radioligand [^{3}H]**5** at 0.5 nM (K_D = 0.56 nM). Competition experiments with human D_{2long}, D_{2short},[37] D_3,[38] and $D_{4.4}$[40] receptors were run with preparations of membranes from CHO cells stably expressing the corresponding receptor and [^{3}H]spiperone at a final concentration of 0.2 nM. The assays were carried out at a protein concentration of 2–6 μg/assay tube and K_D values of 0.091, 0.090, 0.11, and 0.15 nM for the D_{2long}, D_{2short}, D_3, and $D_{4.4}$ receptors, respectively. 5-HT and α_1 receptor binding experiments were performed with homogenates prepared from porcine cerebral cortex as described.[41] Assays were run with membranes at a protein concentration per each assay tube of 80, 110, and 40 μg/mL for 5-HT_{1A}, 5-HT_2, and α_1 receptor, respectively, and radioligand concentrations of 0.2 nM for [^{3}H]prazosin, 0.5 nM for [^{3}H]ketanserin, and 0.3 nM for [^{3}H]**4** with K_D values of 0.30 nM for 5-HT_{1A}, 0.71 nM for 5-HT_2, and 0.16 nM for the α_1 receptor. Protein concentration was established by the method of Lowry using bovine serum albumin as standard.[52]

Mitogenesis Assay. Determination of the intrinsic activity of the representative compound at the dopamine $D_{4.2}$ receptor was carried out by measuring the incorporation of [^{3}H]thymidine into growing cells after stimulation with the test compound as described in the literature.[42,53] For this assay $D_{4.2}$ expressing CHO10001 cells have been incubated with 0.02 μCi [^{3}H]thymidine per well (specific activity of 25 μCi/mmol, Biotrend, Cologne, Germany). The data of four dose response experiments for each compound have been normalized and pooled to get mean values for each concentration tested. These data showed a neutral antagonist effect for each compound compared to the effects of the full agonist quinpirole.

Data Analysis. The resulting competition curves of the receptor binding experiments were analyzed by nonlinear regression using the algorithms in PRISM 3.0 (GraphPad Software, San Diego, CA). The data were fitted using a sigmoid model to provide an IC_{50} value, representing the concentration corresponding to 50% of maximal inhibition. IC_{50} values were transformed to K_i values according to the equation of Cheng and Prusoff.[54]

As a reference, binding curves resulting from the mitogenesis assay with the full agonist quinpirole were analyzed by nonlinear regression. All data of the reference and of the test compounds were normalized (basal effect of 0%; maximum effect of the full agonist quinpirole of

100%) and then combined to get mean values. If an agonist effect was detectable, nonlinear regression analysis of the resulting curve provided the EC_{50} value representing the concentration corresponding to 50% of maximal stimulation as a measure of potency.

Determination of Partition Coefficients (log $P_{7.4}$). By use of the HPLC method corresponding to the OECD guideline for the testing of chemicals,[46] the lipophilicity of compounds was determined using a LiChrospher 100 RP-8 (5 mm) column (Merck). As eluent, Soerensen buffer was used (methanol/phosphate buffer, 75:25 (v/v), at a pH of 7.4). The retention times of a number of reference compounds (ascorbic acid, benzaldehyde, anisole, toluene, 4-bromoanisole, 4-iodoanisole) with known log P values (ranging from −1.67 to 3.24) were determined and the capacity factors k' calculated. Plotting log k' against log P gave the reference curve used to determine the log P values of **3a**−**d** by their respective retention times.

By use of the shake flask method corresponding to the OECD guideline for the testing of chemicals,[46] the lipophilicity of ligands was determined by analyzing the partitioning of the ^{18}F-labeled products between a phosphate buffer (pH 7.4) and an *n*-octanol phase. Then 4.5 μL of the pure ^{18}F-labeled substance in absolute ethanol was added to a mixture of 1.5 mL of phosphate buffer and 150 μL of *n*-octanol. The system was shaken for 3 min and afterward centrifuged for 5 min at 130 00 rpm. On a silica TLC plate, 2.5 μL of the organic phase and 5 μL of the buffer phase were stippled four times, respectively. Partitioning of radioactivity in both phases was determined via an instant imager.

Animals. The 4−6 month old Wistar rats (230−250 g body weight) and 2−6 month old female NMRI mice were purchased from Charles River Laboratories (Wilmington, MA). All animals were kept under a natural light/dark cycle and had access to water and food ad libitum. The local government approved all procedures according to the German Law on the Protection of Animals (sections 7−9 TierSchG). Animal experiments were also approved by the Animal Research Committee of the Scientific and Technical Advisory Board of the Research Center Jülich, Germany. For conducting of ex vivo experiments with living animals, the number for approval was AZ 9.93.2.10.35.07.244.

In Vitro Autoradiography of Rat and Mouse Brain Slices. After the animals were sacrificed, whole brains were rapidly removed and immediately frozen at −80 °C until use. Rat brain sections were prepared in a cryostat microtome (CM 3050, Leica, section thickness 20 μm) at −20 °C, thaw-mounted onto silica-coated object slides dried on silica gel overnight at 4 °C, and stored at −80 °C until use.

Incubation conditions for in vitro autoradiography of all tested substances were similar to those previously described by Zhang et al.[55] All incubations were performed at 22 °C in Tris-HCl buffer (50 mmol/L, pH 7.4). After preincubation in buffer for 10 min rat brain slices were incubated in 5 nmol/L [^{18}F]**3a** or [^{18}F]**3b** or [^{18}F]**3d** or 10 nmol/L [^{18}F]**3c** and mouse brain slices in 20 nmol/L [^{18}F]**3d** for 30 min either with 10 μmol/L displacer (spiperone or cold standard) or with the same amount of DMSO, respectively. They were washed twice for 5 min in ice-cold buffer, rapidly rinsed in ice-cold distilled water, and placed under a stream of dry air for rapid drying. Object slides were exposed to a γ-sensitive film for 15−30 min and laser scanned by a phosphor imager BAS 5000 (Fuji). The evaluation of receptor autoradiography was processed according to standard image analysis software (AIDA 2.31; Raytest Isotopenmeßgeräte, Germany). Nonspecific binding was defined as the residual activity in the presence of cold standard. Specific binding was calculated as the difference between total and nonspecific binding.

Mouse ex Vivo Biodistribution Studies. About 1.1−2.6 MBq [^{18}F]**3d** with a molar activity of 40 GBq/μmol in 50 μL of saline (containing 1% Tween 80) was injected to the tail vain of female NMRI mice. Animals were killed by cervical dislocation at selected times after injection, and organs were removed immediately. All organs and blood were weighed, and the radioactivity was measured in a γ-counter (Auto-Gamma MINAXI 5000 Packard). Brains were fast frozen at −80 °C and cut into horizontal or sagittal sections (thickness, 40 μm) at −20 °C.

In Vivo Stability of 1-(2,3-Dihydrobenzo[*b*][1,4]dioxin-6-yl)-4-((6-[^{18}F]fluoropyridin-3-yl)methyl)piperazine ([^{18}F]3d). In order to determine the stability of [^{18}F]**3d** in mouse serum, removed blood was centrifuged for separation of the plasma which was deproteinated with 2 or 9 volumes of acetonitrile. Samples of 2.5 μL were taken from the extract and analyzed via radio-TLC using ethyl acetate/methanol/diethylamine (96:2:2). In order to estimate the recovery of [^{18}F]**3d** in the extracted solution and to exclude loss of original ligand or possible metabolites, samples of 2.5 μL of origin blood and plasma were submitted to TLC analysis (ethyl acetate/methanol/diethylamine, 96:2:2): R_f = 0.82 ([^{18}F]**3d**); R_f = 0−0.2 ([^{18}F]metabolites).

For the determination of possible cerebral metabolites, mouse brain (n = 3) was homogenized with a Potter Elvehjem homogenizer and treated, as described above, with 9 volumes of acetonitrile.

Staining of Brain Slices by Cresyl Violet. After total decay of the fluorine-18 in the brain sections, cresyl violet staining of cell nuclei of these sections was performed to identify the different brain regions. After fixation with neutral buffered formalin for 30 min at 4 °C the sections were rinsed twice with water and thereafter incubated in cresyl violet solution (40 mM sodium acetate in 10% glacial acetic acid) for 30 min at 60 °C. After a short water rinse the sections were dehydrated by 70%, 80%, 90%, and 100% of ethanol followed by a xylol bath, each step for 5 min. The staining was sealed with DPX Mountant for histology (Fluka).

AUTHOR INFORMATION

Corresponding Author

*Phone: +49 2461 614141. Fax: +49 2461 612535. E-mail: h.h.coenen@fz-juelich.de.

ACKNOWLEDGMENTS

The authors thank Dr. M. Holschbach and Dr. D. Bier, both at INM-5, for performing NMR and MS spectra and for excellent help and discussions on synthetic and pharmacological concerns, Dr. S. Wilbold and Dr. J. Bachhausen, both of Central Institute of Chemical Analysis, Forschungszentrum Jülich, Germany, for performing NMR spectra and elemental analysis, respectively. This work was supported by the Deutsche Forschungsgemeinschaft (DFG, Grant PR 677/2-3).

ABBREVIATIONS USED

5-HT, 5-hydroxytryptamine; CA, cornu ammonis; CHO, Chinese hamster ovary; CoMFA, comparative molecular field analysis; DR, dopamine receptor; GD, gyrus dentatus; GPCR, G-protein-coupled receptor; HPLC, high performance liquid chromatography; ID, injection dose; iv, intravenous; MS, mass spectrometry; nca, no-carrier-added; NMR, nuclear magnetic resonance; NMRI, Navy Medical Research Institute; OECD, Organization for Economic Cooperation and Development; PET, positron emission tomography; pi, postinjection; RCY, radiochemical yield; SAR, structure−activity-relationship; SPECT, single photon emission computer tomography; TLC, thin layer chromatography

REFERENCES

(1) Van Tol, H. H. M.; Bunzow, J. R.; Guan, H.-C.; Sunahara, R. K.; Seemann, P.; Niznik, H. B.; Civelli, O. Cloning of the gene for a human D_4 receptor with high affinity for the antipsychotic clozapine. *Nature* **1991**, *350*, 610−614.

(2) Lahti, R. A.; Evans, D. L.; Stratmann, N. C.; Figur, L. M. Dopamine D_4 versus D_2 receptor selectivity of dopamine receptor antagonists: possible therapeutic implications. *Eur. J. Pharmacol.* **1993**, *236*, 483−486.

(3) Van Tol, H. H.; Wu, C. M.; Guan, H.-C.; Ohara, K.; Bunzow, J. R.; Civelli, O.; Kennedy, J.; Seeman, P.; Niznik, H. B.; Jovanovic, V.

Multiple dopamine D_4 receptor variants in the human population. *Nature* **1992**, *358*, 149−152.
(4) Wang, E.; Ding, Y. C.; Flodman, P.; Kidd, J. R.; Kidd, K. K.; Grady, D. L.; Ryder, O. A.; Spence, M. A.; Swanson, J. M.; Moyzis, R. K. The genetic architecture of selection at the human dopamine receptor D_4 (DRD4) gene locus. *Am. J. Hum. Genet.* **1992**, *74*, 931−944.
(5) Lahti, R. A.; Roberts, R. C.; Cochrane, E. V.; Primus, R. J.; Gallager, D. W.; Conley, R. R.; Tamminga, C. A. Direct determination of dopamine D_4 receptors in normal and schizophrenic postmortem brain tissue: a [^{3}H]NGD-94-1 study. *Mol. Psychiatry* **1998**, *3*, 528−533.
(6) Primus, R. J.; Thurkauf, A.; Xu, J.; Yevich, E.; McInerney, S.; Shaw, K.; Tallman, J. F.; Gallager, D. W. Localization and characterization of dopamine D_4 binding sites in rat and human brain by use of the novel, D_4 receptor-selective ligand ^{3}H-NGD 94-1. *J. Pharmacol. Exp. Ther.* **1997**, *282*, 1020−1027.
(7) Noaín, D.; Avale, M. E.; Wedemeyer, C.; Calvo, D.; Peper, M.; Rubinstein, M. Identification of brain neurons expressing the dopamine D_4 receptor gene using BAC transgenic mice. *Eur. J. Neurosci.* **2006**, *24*, 2429−2438.
(8) Oak, J. N.; Oldenhof, J.; Van Tol, H. H. The dopamine D(4) receptor: one decade of research. *Eur. J. Pharmacol.* **2000**, *405*, 303−327.
(9) Matsumatu, M.; Hidaka, K.; Tada, S.; Tasaki, Y.; Yamaguchi, T. Full-length cDNA cloning and distribution of human dopamine D_4 receptor. *Mol. Brain Res.* **1995**, *29*, 157−162.
(10) Lidow, M. S.; Wang, F.; Cao, Y.; Goldman-Rakic, P. S. Layer V neurons bear the majority of mRNAs encoding the five distinct dopamine receptor subtypes in the primate prefrontal cortex. *Synapse* **1998**, *28*, 10−20.
(11) Ariano, M. A.; Wang, J.; Noblett, K. L.; Larson, E. R.; Sibley, D. R. Cellular distribution of the rat D_4 dopamine receptor protein in the CNS using anti-receptor antisera. *Brain Res.* **1997**, *752*, 26−34.
(12) Helmeste, D. M.; Tang, S. W.; Bunney, W. E. Jr.; Potkin, S. G.; Jones, E. G. Decrease in sigma but no increase in striatal dopamine D_4 sites in schizophrenic brains. *Eur. J. Pharmacol.* **1996**, *314*, R3−5.
(13) Reynolds, G. P.; Mason, S. L. Absence of detectable striatal dopamine D4 receptors in drug-treated schizophrenia. *Eur. J. Pharmacol.* **1995**, *281*, R5−R6.
(14) Prante, O.; Dörfler, M.; Gmeiner, P. Dopamine Receptor Subtyp-Selective Drugs: D_2-like Receptors. In *The Dopamine Receptors*, 2nd ed.; Neve, K. A., Ed.; Humana Press, Springer Verlag: Heidelberg, Germany, 2010.
(15) Löber, S.; Hübner, H.; Tschammer, N.; Gmeiner, P. Recent advances in the search for D_3- and D_4-selective drugs: probes, models and candidates. *Trends Pharmacol. Sci.* **2011**, *32*, 148−157.
(16) Glase, S. A.; Akunne, H. C.; Georgic, L. M.; Heffner, T. G.; MacKenzie, R. G.; Manley, P. J.; Pugsley, T. A.; Wise, L. D. Substituted [(4-phenylpiperazinyl)-methyl]benzamides: selective dopamine D_4 agonists. *J. Med. Chem.* **1997**, *40*, 1771−1772.
(17) Löber, S.; Hübner, H.; Utz, W.; Gmeiner, P. Rationally based efficacy tuning of selective dopamine D_4 receptor ligands leading to the complete antagonist 2-[4-(4-chlorophenyl)piperazine-1-yl]methylpyrazol[1,5-*a*]pyridine (FAUC 213). *J. Med. Chem.* **2001**, *44*, 2691−2694.
(18) Nakane, M.; Cowart, M. D.; Hsieh, G. C.; Miller, L.; Uchic, M. E.; Chang, R.; Terranova, M. A.; Donnelly-Roberts, D. L.; Namovic, M. T.; Miller, T. R.; Wetter, J. M.; Marsh, K.; Stewart, A. O.; Brioni, J. D.; Moreland, R. B. 2-[4-(3,4-Dimethylphenyl)piperazin-1-ylmethyl]-1*H*-benzoimidazole (A-381393), a selective dopamine D_4 receptor antagonist. *Neuropharmacology* **2005**, *49*, 112−121.
(19) Lanig, H.; Utz, W.; Gmeiner, P. Comparative molecular field analysis of dopamine D_4 receptor antagonists including 3-[4-(4-chlorophenyl)piperazin-1-ylmethyl]pyrazolo[1,5-*a*]pyridine (FAUC 113), 3-[4-(4-chlorophenyl)piperazin-1-ylmethyl]-1*H*-pyrrolo-[2,3-*b*]pyridine (L-745,870), and clozapine. *J. Med. Chem.* **2001**, *44*, 1151−1157.
(20) Ben Zion, I. Z.; Tessler, R.; Cohen, L.; Lerer, E.; Raz, Y.; Bachner-Melman, R.; Gritsenko, I.; Nemanov, L.; Zohar, A. H.; Belmaker, R. H.; Benjamin, J.; Ebstein, R. P. Polymorphisms in the dopamine D_4 receptor gene (*DRD4*) contribute to individual differences in human sexual behavior: desire, arousal and sexual function. *Mol. Psychiatry* **2006**, *11*, 782−786.
(21) Melis, M. R.; Succu, S.; Mascia, M. S.; Argiolas, A. PD-168077, a selective dopamine D_4 receptor agonist, induces penile erection when injected into the paraventricular nucleus of male rats. *Neurosci. Lett.* **2005**, *379*, 59−62.
(22) Rondou, P.; Haegeman, G.; Van Craenenbroeck, K. The dopamine D_4 receptor: biochemical and signalling properties. *Cell. Mol. Life Sci.* **2010**, *67*, 1971−1986.
(23) Hsieh, G. C.; Hollingsworth, P. R.; Martino, B.; Chang, R.; Terranova, M. A.; O'Neill, A. B.; Lynch, J. J.; Moreland, R. B.; Donnelly-Roberts, D. L.; Kolasa, T.; Mikusa, J. P.; McVey, J. M.; Marsh, K. C.; Sullivan, J. P.; Brioni, J. D. Central mechanisms regulating penile erection in conscious rats: the dopaminergic systems related to the proerectile effect of apomorphine. *J. Pharmacol. Exp. Ther.* **2004**, *308*, 330−338.
(24) Matulenko, M. A.; Surber, B.; Fan, L.; Kolasa, T.; Nakane, M.; Terranova, M. A.; Uchic, M. E.; Miller, L. N.; Chang, R.; Donnelly-Roberts, D. L.; Namovic, M. T.; Moreland, R. B.; Brioni, J. D.; Stewart, A. O. Synthesis and activity of 2-[4-(4-[^{3}H]-2-cyanophenyl)piperazinyl]-*N*-(2,4,6-[^{3}H]$_3$-3-methylphenyl)acetamide: a selective dopamine D_4 receptor agonist and radioligand. *Bioorg. Med. Chem. Lett.* **2004**, *14*, 5095−5098.
(25) Boy, C.; Klimke, A.; Holschbach, M.; Herzog, H.; Mühlensiepen, H.; Rota Kops, E.; Sonnenberg, F.; Gaebel, W.; Stöcklin, G.; Markstein, R.; Müller-Gärtner, H. W. Imaging dopamine D_4 receptors in the living primate brain: a positron emission tomography study using the novel D_1/D_4 antagonist [^{11}C]SDZ GLC 756. *Synapse* **1998**, *30*, 341−350.
(26) Zhang, M. R.; Haradahira, T.; Maeda, J.; Okauchi, T.; Kawabe, K.; Noguchi, J.; Kida, T.; Suzuki, K.; Suhara, T. Syntheses and pharmacological evaluation of two potent antagonists for dopamine D_4 receptors: [^{11}C]YM-50001 and *N*-[2-[4-(4-Chlorophenyl)-piperizin-1-yl]ethyl]-3-[^{11}C]methoxybenz-amide. *Nucl. Med. Biol.* **2002**, *29*, 233−241.
(27) Oh, S. J.; Lee, K. C.; Lee, S. Y.; Ryu, E. K.; Saji, H.; Choe, Y. S.; Chi, D. Y.; Kim, S. E.; Lee, J.; Kim, B. T. Synthesis and evaluation of fluorine-substituted 1*H*-pyrrolo[2,3-*b*]pyridine derivatives for dopamine D_4 receptor imaging. *Bioorg. Med. Chem.* **2004**, *12*, 5505−5513.
(28) Kortagere, S.; Gmeiner, P.; Weinstein, H.; Schetz, J. A. Certain 1,4-disubstituted aromatic piperidines and piperazines with extreme selectivity for the dopamine D_4 receptor interact with a common receptor microdomain. *Mol. Pharmacol.* **2004**, *66*, 1491−1499.
(29) Wang, Y.; Mathis, C. A.; Huang, G. F.; Debnath, M. L.; Holt, D. P.; Shao, L.; Klunk, W. E. Effects of lipophilicity on the affinity and nonspecific binding of iodinated benzothiazole derivatives. *J. Mol. Neurosci.* **2003**, *20*, 255−260.
(30) Sebai, S.; Baciu, M.; Ces, O.; Clarke, J.; Cunningham, V.; Gunn, R.; Law, R.; Mulet, X.; Parker, C.; Plisson, C.; Templer, R.; Gee, A. To lipophilicity and beyond: towards a deeper understanding of radioligand non-specific binding. *NeuroImage* **2006**, *31*, T44−T186.
(31) Wilson, A.; Garcia, A.; Chestakova, A.; Houle, S. How good is the correlation between lipophilicity/phospholipicity and non-specific binding. *NeuroImage* **2004**, *22*, T61−T200.
(32) Blom, E.; Karimi, F.; Eriksson, O.; Hall, H.; Långström, B. Synthesis and in vitro evaluation of ^{18}F-β-carboline alkaloids as PET ligands. *J. Labelled Compd. Radiopharm.* **2008**, *51*, 277−282.
(33) Hodgetts, K. J.; Kieltyka, A.; Brodbeck, R.; Tran, J. N.; Wasley, J. W.; Thurkauf, A. 6-(4-Benzylpiperazin-1-yl)benzodioxanes as selective ligands at cloned primate dopamine D(4) receptors. *Bioorg. Med. Chem.* **2001**, *9*, 3207−3213.
(34) Prante, O.; Tietze, R.; Hocke, C.; Löber, S.; Hübner, H.; Kuwert, T.; Gmeiner, P. Synthesis, radiofluorination, and in vitro evaluation of pyrazolo[1,5-*a*]pyridine-based dopamine D_4 receptor

ligands: discovery of an inverse agonist radioligand for PET. *J. Med. Chem.* **2008**, *51*, 1800−1810.
(35) Liu, K. G.; Robichaud, A. J. A general and convenient synthesis of *N*-aryl piperazines. *Tetrahedron Lett.* **2005**, *46*, 7921.
(36) Kügler, F.; Ermert, J.; Coenen, H. H. Labeling of a series of benzodioxine piperazines with fluorine-18 as promising selective radioligands for imaging dopamine D_4 receptors. Unpublished results.
(37) Hayes, G.; Biden, T. J.; Selbie, L. A.; Shine, J. Structural subtypes of the dopamine D_2 receptor are functionally distinct: expression of the cloned D2A and D2B subtypes in a heterologous cell line. *Mol. Endocrinol.* **1992**, *6*, 920−926.
(38) Sokoloff, P.; Giros, B.; Martres, M. P.; Bouthenet, M. L.; Schwartz, J. C. Molecular cloning and characterization of a novel dopamine receptor (D_3) as a target for neuroleptics. *Nature* **1990**, *347*, 146−151.
(39) Asghari, V.; Sanyal, S.; Buchwaldt, S.; Paterson, A.; Jovanovic, V.; Vantol, H. H. M. Modulation of intracellular cyclic-Amp levels by different human dopamine D4 receptor variants. *J. Neurochem.* **1995**, *65*, 1157−1165.
(40) Hübner, H.; Haubmann, C.; Utz, W.; Gmeiner, P. Conjugated enynes as nonaromatic catechol bioisosteres: synthesis, binding experiments, and computational studies of novel dopamine receptor agonists recognizing preferentially the D_3 subtype. *J. Med. Chem.* **2000**, *43*, 756−762.
(41) Schlotter, K.; Boeckler, F.; Hübner, H.; Gmeiner, P. Fancy bioisosteres: metallocene-derived G-protein-coupled receptor ligands with subnanomolar binding affinity and novel selectivity profiles. *J. Med. Chem.* **2005**, *48*, 3696−3699.
(42) Hübner, H.; Kraxner, J.; Gmeiner, P. Cyanoindole derivatives as highly selective dopamine D_4 receptor partial agonists: solid-phase synthesis, binding assays, and functional experiments. *J. Med. Chem.* **2000**, *43*, 4563−4569.
(43) Chio, C. L.; Lajiness, M. E.; Huff, R. M. Activation of heterologously expressed D_3 dopamine receptors: comparison with D_2 dopamine receptors. *Mol. Pharmacol.* **1994**, *45*, 51−60.
(44) *MarvinSketch Demo*, version 5.1.4; ChemAxon: Budapest, Hungary, 2009; http://www.chemaxon.com/marvin/sketch/index.jsp.
(45) *ALOGPS*, version 2.1; Virtual Computational Chemistry Laboratory, 2009; www.vcclab.org/lab/alogps/start.html
(46) *OECD Guideline for the Testing of Chemicals*; OECD: Paris, France, 1989; http://www.oecd.org/dataoecd/17/36/1948177.pdf.
(47) Mendel, C. M.; Mendel, D. B. "Non-specific" binding. *Biochem. J.* **1985**, *228*, 269−272.
(48) Prante, O.; Hocke, C.; Löber, S.; Hübner, H.; Gmeiner, P.; Kuwert, T. Tissue distribution of radioiodinated FAUC113. *Nuklearmedizin* **2006**, *45*, 41−48.
(49) Rubi, B.; Ljubicic, S.; Pournourmohammadi, S.; Carobbio, S.; Armanet, M.; Bartley, C.; Maechler, P. Dopamine D_2-like receptors are expressed in pancreatic beta cells and mediate inhibition of insulin secretion. *J. Biol. Chem.* **2005**, *280*, 36824−36832.
(50) Qaim, S. M.; Clark, J. C.; Crouzel, C.; Guillaume, M.; Helmecke, H. J.; Nebeling, B.; Pike, V. W.; Stöcklin, G. In *Radiopharmaceuticals for PET*; Stöcklin, G., Pike, V. W., Eds.; Kluwer Academic Publishers, Dordrecht, The Netherlands, 1993; pp 15−26.
(51) Coenen, H. H.; Schüller, M.; Stöcklin, G.; Klatte, B.; Knöchel, A. Preparation of N.C.A. [17-^{18}F]-fluoroheptadecanoic acid in high yields via aminopolyether supported, nucleophilic fluorination. *J. Labelled Compd. Radiopharm.* **1986**, *23*, 455−466.
(52) Lowry, O. H.; Rosebrough, N. J.; Farr, A. L.; Randall, R. J. Protein measurement with the Folin phenol reagent. *J. Biol. Chem.* **1951**, *193*, 265−275.
(53) Mierau, J.; Schneider, F. J.; Ensinger, H. A.; Chio, C. L.; Lajiness, M. E.; Huff, R. M. Pramipexole binding and activation of cloned and expressed dopamine D_2, D_3 and D_4 receptors. *Eur. J. Pharmacol.* **1995**, *290*, 29−36.
(54) Cheng, Y.; Prusoff, W. H. Relationship between the inhibition constant (K_i) and the concentration of inhibitor which causes 50% inhibition (IC_{50}) of an enzymatic reaction. *Biochem. Pharmacol.* **1973**, *22*, 3099−3108.
(55) Zhang, K.; Weiss, N. T.; Tarazi, F. I.; Kula, N. S.; Baldessarini, R. J. Effects of alkylating agents on dopamine D(3) receptors in rat brain: selective protection by dopamine. *Brain Res.* **1999**, *847*, 32−37.